LAWRENCE
LIVERMORE
NATIONAL
LABORATORY

LLNL-TR-520260

Observations and Modeling of Long Negative Laboratory Discharges:

Identifying the Physics Important to an Electrical Spark in Air

Christopher J. Biagi
University of Florida

Professor Martin Uman
Advisor, University of Florida

10 November 2011

For questions
please call Mike Ong or Mike Perkins
Lawrence Livermore National Laboratory

Auspices

This work performed under the auspices of the U.S. Department of Energy by Lawrence Livermore National Laboratory under Contract DE-AC52-07NA27344.

Final Report to University of California, Lawrence Livermore National Laboratory
Grant DE-AC52-07NA27344
1/25/2011 – 9/30/2011

Observations and Modeling of Long Negative Laboratory Discharges: Identifying the Physics Important to an Electrical Spark in Air

by

Christopher J. Biagi

10 November 2011

1. Introduction

There are relatively few reports in the literature focusing on negative laboratory leaders. Most of the reports focus exclusively on the simpler positive laboratory leader that is more commonly encountered in high voltage engineering [*Gorin et al.*, 1976; *Les Renardieres Group*, 1977; *Gallimberti*, 1979; *Domens et al.*, 1994; *Bazelyan and Raizer* 1998]. The physics of the long, negative leader and its positive counterpart are similar; the two differ primarily in their extension mechanisms [*Bazelyan and Raizer*, 1998]. Long negative sparks extend primarily by an intermittent process termed a 'step' that requires the development of secondary leader channels separated in space from the primary leader channel. Long positive sparks typically extend continuously, although, under proper conditions, their extension can be temporarily halted and begun again, and this is sometimes viewed as a stepping process. However, it is emphasized that the nature of positive leader stepping is not like that of negative leader stepping.

There are several key observational studies of the propagation of long, negative-polarity laboratory sparks in air that have aided in the understanding of the stepping mechanisms exhibited by such sparks [e.g., *Gorin et al.*, 1976; *Les Renardieres Group*, 1981; *Ortega et al.*, 1994; *Reess et al.*, 1995; *Bazelyan and Raizer*, 1998; *Gallimberti et al.*, 2002]. These reports are reviewed below in Section 2, with emphasis placed on the stepping mechanism (the space stem, pilot, and space leader). Then, in Section 3, reports pertaining to modeling of long negative leaders are summarized.

2. Overview of Long Negative Leaders

The negative polarity discharge begins at the cathode with the formation of corona streamers (filamentary channels of low conductivity) [*Loeb and Meek*, 1941; *Raether*, 1964] that begin when one or more free electrons appear near the cathode and within the volume (called the critical volume by *Gallimberti* [1979], and the ionization zone by *Bazelyan and Raizer* [1998]) where the convergent electric field is on the order of 30 kV cm^{-1} or more. The initial free electrons are produced by any of several processes, such as, photoionization, radioactive decay, and cosmic rays. The field value at which breakdown occurs, or the inception field, generally depends on the electrode geometry, the gap distance, and the ambient air pressure [e.g., *Peek*, 1929; *Les Renardieres Group*, 1972]. Similarly, the inception voltage, defined as the voltage at which the first corona streamer burst appears, is to some extent random, and it depends on the voltage rise time and the electrode geometry [*Bazelyan et al.*, 1961; *Les Renardieres Group*, 1981].

The initial free electrons gain more energy from the electric field than they lose through interactions with the gaseous medium of the gap, causing them to accelerate away from the cathode. As the electrons gain energy, they generate additional electrons via impact ionization. These new electrons experience a similar acceleration and energy gain, thereby generating new electrons, resulting in electron avalanche breakdown. Electron emissions from the cathode occuring via ion impact or photo ionization generate further electron avalanche breakdown. Additionally, depending on the gaseous medium, a wide range of chemical reactions can occur that have influence on the ion and electron density. Detailed descriptions of the chemistry of corona streamers can be found in the literature [e.g., *Gallimberti*, 1979; *Les Renardieres Group*, 1981; *Wang and Kunhardt*, 1990; *Alexandrov and Bazelyan*, 1996; *Marrow and Lowke*, 1997;

Alexandrov and Bazelyan,1999; *Nudnova and Starikovskii*, 2008; *Winands et al.*, 2008; *Nguyen et al*, 2010].

Corona streamers consist of thousands of electron avalanches that extend to several tens of centimeters to meters in length [e.g., *Les Renardieres Group*, 1981; *Reess et al.*, 1995]. The mean charge injected into gaps by the first corona bursts ranges from 10^{-7} to 10^{-6} C [e.g., *Les Renardieres Group*, 1981; *Ortega et al.*, 2005]. The corona streamers push electrons from the vicinity of the electrode, and build up a positive space charge which produces a field reduction [e.g., *Trichel*, 1938; *Les Renardieres Group*, 1981]. Under certain conditions, the build up of positive space charge near the cathode cause the negative corona streamers to develop in a pulsed manner (Trichel pulses) with a frequency on the order of tens to a hundred MHz [*Trichel*, 1938; *Reess et al.*, 1995].

Bazelyan et al. [1961] examined the relationship between the voltage rise time and breakdown voltage for 'oblique' voltage rises (steady exponential increase). The breakdown voltage varies with voltage rise time with an asymmetric 'U curve' shape with a minimum value. The minimum value has slight dependence on gap length (curves for 1-3.75 m are shown), but is generally within the range of 150-180 μs. The breakdown voltage is much lower for "switching surges" having rise times within this range compared to DC or AC voltage application (which can be viewed as the limiting cases of the voltage rise time). The increasing breakdown voltage for decreasing voltage rise times (the left side of the U curve) is a result of the discharge being slower than the rate of voltage rise. The increasing breakdown voltage for increasing voltage rise times (the right side of the U curve) is a result of the build up of space charge in the vicinity of the electrode. Similar U curves have been reported for different gap configurations by others [e.g., *Les Renardieres Group* 1981]

As long as the applied voltage is sufficiently high (the level depends on the gap geometry and the gas-medium thermodynamics), the corona streamers will continue to develop, forming a current that will cause the gas temperature to increase as a result of the Joule heating. The next step in the leader formation is the development of one or more 'stems' (sometime called space stems if they form unattached to an electrode). *Reess et al*. [1995] performed an observational study of space stem formation in discharges in a 1.3 m point-to-plane gap, which is summarized in the following text. *Reess et al.* [1995] observed that the first space stems form in the vicinity of the cathode (where negative corona streamers previously formed) with the inception of retrograde positive streamers from luminous spots that apparently contain excess positive ions. The luminous spots correspond to the branching points of the original negative corona streamers. The retrograde positive streamers contact the cathode and bring forward the cathode's potential, and supply the stem with new electrons. The newly supplied electrons allow the formation of new negative streamers from the space stem that extend further into the gap. *Reess et al.* [1995] determined that about 300 nC of charge must be transferred to the stem before new negative streamers can develop. In the new corona streamers, new space stems form at the branching points. Retrograde positive streamers again extend toward the cathode from these new space stems (and through the previous space stem and positive streamers), in effect 'moving' the space stem further into the gap in an intermittent manner. This sequence occurs every few hundred nanoseconds [e.g., *Gorin et al.*, 1976; *Reess et al.*, 1995]. The space stem and its associated positive and negative streamers is sometimes called a 'pilot' [*Bacchiega et al.*, 1994]. *Les Renardieres Group* [1981], *Ortega et al.* [1994], and *Reess et al* [1995] all report a similar 'equivalent velocity' for the space stem motion of 1×10^6 m s^{-1}.

The corona streamer currents that are rooted at the stem region (estimated to have a volume of about 1 cm^3 by *Gorin et al.* [1976]) increase the local thermal energy, producing significant effects, including: (1) a temperature increase of the gas and plasma by Joule heating from about 300 K to 1500 K, (2) a hydrodynamic expansion and reduction in gas density, (3) a increase in the reduced electric field (the electric field normalized to the density of neutral particles), (4) a sharp increase the conductivity of the stem, and (5) an increase in the electric field at the stem tips. When the temperature in a stem reaches a critical temperature of about 1500 K, there is a sudden and significant increase in the electron density due to negative ions abruptly releasing their captured electrons. This sudden release of electrons results in an abrupt and large increase in the space stem plasma conductivity. The larger increase in plasma conductivity marks the transition of the space stem to a space leader

The space leader elongates bi-directionally from a space stem's location. The upper tip of the space leader is positively charged, and it extends toward the cathode. The bottom tip of the space leader is negatively charged, and it extends into the gap. The longitudinal current in the space leader is confined to a diameter between 0.5 mm and a 4 mm (the current diameter increases in time due to hydrodynamic expansion). *Ortega et al.* [1994], studying negative discharges in a 16.7-m gap, observed that the space stem became a space leader when it was typically between 1.4 to 2.2 m in front of the cathode or primary leader channel. It can be presumed that the space leader will be unable to form in gaps shorter than 1.4 m. The number of steps in *Ortega et al.'s* 16.7-m gap ranged from 4 to 7, which is higher than the number steps than was observed by *Les Renardieres Group* [1981] in 5 and 7 m gaps, 2 to 5 steps. *Ortega et al.* [1994] observed that for identical air conditions, the leader-path length increases with the

time to peak of the voltage impulse, and they noted a linear correlation between the number of steps and gap length.

Ortega et al. [1994] observed in their streak photographs that the elongation of the leader channel with each step ranged from 1 to 5 m, and the time between elongations (the completion of steps) ranged from 10-50 μs. They did not find relationship between the step length and interstep times, but instead noted that the times at which steps occur are 'quite random'. In a "withstand" case, they observed that the discharge ended with a space stem and space leader that failed to produce a new step. Simultaneous UV and IR photomultiplier measurements revealed that IR emission occurs only during restrikes (the connection of space leader and primary leader), while UV emission occurs throughout, most notably between restrikes when primarily streamers are propagating. They observed space leaders forming in series to produce a longer step, and in parallel to produce branching. Further, their observations indicated that for a space stem to become a space leader, an addition space stem 'downstream' must develop.

Ortega et al. [1994] gave estimations of the elongation speeds for the primary leader and space leader, and the propagation speed of the space stem, when the overall leader was less than 5 m in length. The speed estimations were apparently made from still photographs obtained with an image converter camera, but the rate at which the photographs were obtained is not stated. The primary leader extended with an estimated mean speed in the range of 1.3 to 2.8 x 10^4 m s^{-1}. The cathode-directed end of the space leader (upper, positively charged end) extended with an estimated mean speed between 3.2 and 4.9 x 10^4 m s^{-1}. The anode-directed end (bottom, negatively charged end) extended with a slower mean speed, between 1.2 and 2.9 x 10^4 m s^{-1}. When the positive end of the space leader merges with the cathode a wave carrying the higher cathode potential travels to the negative end of the space leader (forming a "step"), where it

creates a relatively large corona streamer burst that contributes to production (heating and charging) of the following step.

Ortega et al. [1994] observed using a shunt in the high-voltage electrode a current pulse with a peak current ranging from 100 to 600 A was associated with each leader step, although they noted that the peak current may have been restricted by the external circuit. The values of peak current did not show a trend from step to step. A step formed by a single space leader will produce a narrow, unipolar current pulse. A step formed by two or more space leaders will produce a multi-peaked, unipolar pulse with a considerably longer width. In Figure 9 of *Ortega et al.* [1994], it appears that there is a current peak for each space leader that contributes to a step. Between 200 and 400 μC of charge flowed from the high voltage electrode with each step, but it is not clear what fraction of this charge contributes to the new step (some charge may be swept away by the high-electric fields in the gap). The charge per unit length for the first four steps was determined to range from 100 to 130 μC m^{-1}.

Ortega et al. [1994] extended the work of *Les Renardieres Group* [1981] in relating the potential of the space stem just before space leader inception, U_{SS}, to the voltage at the leader inception from the high voltage electrode, U_1. The value of U_{SS} was calculated using the following relation:

$$U_{SS} = U_P - E_{L-}L_- - E_{S+}L_{S+} \qquad 1\text{-}1$$

where U_P is the peak high voltage electrode potential, L_- is the length of the negative (primary) leader, L_{S+} is the length of the positive corona streamers connecting the space stem to the negative leader, E_{L-} is the electric field in the negative (primary) leader (determined graphically from Figure 6.5.2 in *Les Renardieres Group* [1981]), and E_{S+} is the electric field of the positive corona streamers (assumed to be 500 kV m^{-1}). The values of U_1 (the cathode potential at leader

inception time) and U_{SS} increase with increasing distance between the high-voltage electrode or space stem and the ground plane (anode), D_{SS}, according to the following relation.

$$U_{SS} = 0.8\left(D_{SS} - 1.5\right)^{0.45} \qquad 1\text{-}2$$

The similarity between U_1 and U_{SS} is an indication that the leader inception from the high voltage electrode is preceded by the formation of a stem on the electrode surface (as opposed to a space stem), as *Bacchiega et al.* [1994] observed. Equation 1-2 is probably only valid for gaps larger than 2 m, since the space leader apparently cannot form in much smaller gaps [*Ortega et al.*, 1994].

Ortega et al. [1994], from the strioscopic measurements, observed that when the leader channel first forms (which they report happens 'quasi-instantaneously'), its diameter is 2 mm, and the diameter increases to 8 mm prior to the final jump. The spark channel is about 2.5 cm in diameter when the current is between 10 and 15 kA. The channel remains hot for some tens of milliseconds.

With a description of the space stem and space leader in hand, we describe schematically in Figure 1 the spatial and temporal development of the long negative laboratory leader during its extension from the cathode, and before the final jump. The diagram in panel A of Figure 1 illustrates the streamer zone containing a pilot of a negative laboratory leader several microseconds after its initiation from the high-voltage electrode, as first described by *Gorin et al.* [1976]: (1) primary leader channel that grows from the negative high-voltage electrode, (2) leader tip, (3) positive streamers emanating from the space stem to the primary leader channel, (4) space stem, and (5) negative streamers emanating from the space stem into the gap. Note that the streamer zone extends from the primary leader channel intermittently [e.g., *Reess et al.*, 1995]. Panel B of Figure 1 depicts negative leader development in time from left to right, as

interpreted via streak photography, with the cathode current is shown below (Figure 1C). The cathode is at the top, and the leader develops downward toward a grounded plane. The processes identified by numbers 1 through 5 in Figure 1B correspond to the descriptions for Figure 1A. The primary leader tip extends quasi-continuously down curve 2 in Figure 1B. The space stem moves along the negatively sloped dashed line labeled 4, and the distance between the primary leader tip and space stem increases with time. The space stem's temperature and conductivity

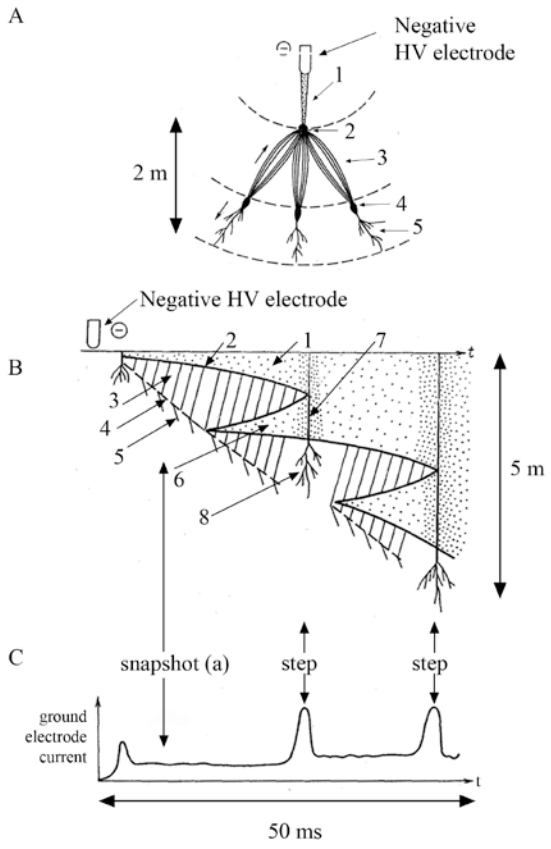

Figure 1. Schematics illustrating the stepped development of the negative leader. (A) Diagram (snapshot) showing the streamer zone structure ahead of a negative leader tip, (B) space-time diagram of negative leader development with time increasing from left to right over 50 μs, (C) the corresponding current in the ground electrode . Diagrams are adapted from *Gorin et al.* [1976].

suddenly increase, causing the stem to become a space leader (6) that develops bi-directionally. Note that one or more space stems can form ahead of (below) the space leader. When the

positive end (top) of the space leader merges with the negative leader tip (at 7), the higher potential of the leader channel is transferred to the negative end of the space leader (bottom), followed by a burst of negative corona streamers (8). At this point, current and luminosity waves propagate up the leader channel, and the leader step has completed its extension of the primary leader channel. The spark propagation continues in the corona created at 8 with the space stem that begins the next leader step. Current pulses in the grounded electrode are associated with each step, shown in panel C of Figure 1.

In long negative laboratory discharges, the negative leader connects to the ground plane (anode) via an upward positive connecting leader in the so-called final jump phase. According to *Les Renardieres Group* [1981], who give the most detailed observational description of the final jump phase, there are three types of final jump mechanisms. In type A, negative corona streamers from a space stem make first contact with the ground plane. Then, the space stem accelerates toward the anode. When the space stem touches the anode, it initiates from the ground plane an upward positive connecting leader that connects to the primary negative leader channel. In type B, a space leader develops between the primary downward negative leader and the upward positive connecting leader. The presence of the space leader alters the characteristics of the upward positive connecting leader. Finally, in type C, which is similar to type A, the burst of negative corona streamers following the connection of a space leader to the primary negative leader channel reaches the anode. An upward positive connecting leader develops toward the negative leader without the presence of a space stem (as was the case for type A).

Les Renardieres Group [1981] observed that, for negative discharges in a 7-m gap, the upward positive leader ranged between 0.7 to 3 m, or 10 to 45% of the gap distance. The duration of the final jump phase is on the order of a few μs, which is shorter than the final jump

phase in positive laboratory discharges. Based on the presence of channel loops, *Ortega et al.* [1994] inferred that the length of the upward positive connecting leaders were about 4 m, or about 24% of the gap length (16.7 m). *Les Renardieres Group* [1981] found that the type A mechanism almost always occurs in gaps of 2 m. For a gap length of 7 m, the type B and type C mechanisms occurred most often. They also found that the height of the final jump mechanism was higher for voltage rise time to crest shorter than the critical value.

Finally, it was been recently discovered [*Dwyer et al.*, 2005] that laboratory sparks produce x-ray emission that is similar to the x-ray emission observed from lightning. *Dwyer et al.* [2005] observed x-rays from positive and negative discharges in a 2-m point-to-plane gap, as well as the gaps in the Marx generator. The deposited x-ray energy ranged from 660 keV to 1.8 MeV for positive discharge, and from 56 keV to 520 keV for negative discharges. The lower energy deposition by negative discharges indicates that negative discharges produce softer (lower energy) x-rays, or they emit fewer x-rays that do positive discharges. The x-ray bursts occurred prior to the high-current arc when the electric fields were highest.

3. Modeling Long Negative Laboratory Leaders

There are only a handful of reports in the literature describing attempts to model the initiation and propagation of long negative laboratory leaders. This section presents summaries of the most relevant reports that have been identified.

3.1 Les Renardieres Group [1981]

Les Renardieres Group [1981] is a comprehensive observational study of the long negative laboratory discharge in gap lengths of 2, 4, 5 and 7 m with different electrode geometries (cone and rod). They give detailed observations of breakdown parameters, first and

second corona streamers forming at the cathode, the leader phase which includes the space stem and space leader, and the final jump. They also present strioscopic and spectroscopic measurements of the discharge processes. They give many empirical expressions, although the scatter in the data from which these expressions are derived tends to be significant, which indicates, as they noted, that there is no 'typical' discharge. Some modeling results are presented, although the modeling itself is not described adequately. A hydrodynamic model is formulated using energy and momentum conservation equations to model the dynamics of neutral species in the leader channel.

Les Renardieres Group [1981] contains a number of 'sub-reports' by various authors that discuss specific aspects of the long negative laboratory discharge. A sub-report authored by *Pigini et al.* evaluates the electric fields in the different discharge phases with the purpose of showing that the space leader forms at the space stem when the stem potential is close to the leader inception voltage at the cathode. Another sub-report, authored by *Hutzler and Kleimaier*, proposes a model to describing the streamer development from the space stem. In their model, the space stem is approximated by two spheres of different size that are separated by a short distance. Each contains a uniform charge distribution, one being positive, and the other being negative (and having more overall charge than the positive sphere). This geometrical configuration essentially approximates the space stem as an uneven electric dipole, which allows for easy calculation of the electric field, and an estimation of the charges involved in the process.

3.2 Rizk [1989]

Rizk [1989] develops analytical expressions to model the continuous leader inception and the breakdown of long air gaps under positive switching impulses. Considering the leader as a cylindrical distribution of space charge, an expression is derived to determined the electric field

at any point between a leader and a ground plane. Equations are derived to predict the voltage required to begin continuous leader in any gap length, and the length of the final jump. These equations are partially based on the experimental results of *Carrara and Thione* [1976]. The expression for the final jump length is similar to an empirical expression given by *Hutzler and Hutzler* [1982] (in French). An expression is derived to predict the voltage drop along a leader that is based on the assumption that the conductivity of the leader channel decays exponentially in time. The leader length and decay time are related by the leader extension speed. The expression yields a similar although slightly smaller voltage drop versus length as an empirical expression given in *Thione* [1979]. The expressions for the critical leader inception voltage and the leader voltage drop are combined to yield expressions for the minimum breakdown voltage of a rod-plane gap that matches very well several observational data of *Les Renardieres Group* [1974] and *Pigini et al.* [1979].

3.3 Fofana and Beroual [1995, 1996a, 1996b, 1997]

Fofana and Beroual have published a series of detailed and well written papers in which they develop a positive polarity discharge model utilizing a distributed RLC circuit that yields the potential drop along the leader channel, the power and energy injected into the gap, and the leader charge, current, and development speed.

Fofana and Beroual [1995] develop an equivalent electrical network of RC nodes to model the evolution of voltage, current, and charge of positive laboratory leaders subjected to an oscillatory voltage impulse. The number of RC nodes is equal to the total leader length (to be simulated) divided by the desired step length. Each RC node has a switch, and in the model the leader growth is 'forced' by closing these switches successively. The time between switch closings is the leader length (arbitrarily set) divided by the leader propagation speed. The

modeled voltage generator is described in detail, and an RLC circuit is described that can produce a bi-exponential impulse with superimposed oscillations. The leader resistance is assumed to be constant and uniform. In order to calculate the per unit length capacitance, it is assumed that the foregoing streamers at the leader tip and the ground electrode are solid angles of two concentric spheres. As the leader extends, the distance between the two concentric spheres decreases, so the per unit length capacitance increases with leader length. The model appears to reproduce well characteristics (voltage, current, total charge) of discharges documented in *Ortega et al*. [1991] and *Ortega* [1992], although the comparison of the model predictions and observations is inadequately described.

Fofana and Beroual [1996a] derive an equation relating the leader development speed to the fraction of input energy that is 'kinetic', i.e. grows the leader channel. Such an equation allows one to model leader channel growth based on the power yielded by an RLC distributed circuit model. It is assumed that the leader radius and temperature are constant, and that the leader pressure is in equilibrium with the ambient air. The equation includes a factor to describe what fraction of the total input energy is spent growing the leader channel, and this factor is determined by calibration with experimental observations.

Fofana and Beroual [1996b] develop what they term a "whole discharge" model that represents with a distributed RLC circuit the positive polarity leader development, final jump, and return stroke. The new distributed circuit model is an extension of their previous RC circuit model that incorporates their leader extension speed model. First corona and streamers are not parts of the model. The distributed circuit provides at each model step the charge, the potential drop along the leader channel, the power and energy injected into the gap, and the leader velocities. The applied voltage impulse is the same bi-exponential with adjustable rise time, fall

time, and time to half value, that is used in *Fofana and Beroual* [1995]. The per unit length resistance during the leader phase is calculated assuming the channel is cylindrical with uniform current. The leader conductivity is taken from measurements by *Les Renardieres Group* [1977], and the channel radius is deduced from experimental data with which the model is tested. For the return stroke per unit length resistance, the cylindrical channel radius is assumed to be constant, and the conductivity is calculated using a relation given by *Gallimberti* [1979]. The leader inductance is neglected. For the return stroke, both the internal and external inductance (per unit length) are calculated geometrically under the assumption that the channel is cylindrical with uniform current. The model is tested by comparing its predictions with two laboratory sparks: one in a 10 m gap reported in *Les Renardieres Group* [1977], and the other in a 16.7 m gap reported in *Domiens* [1987]. For both cases, the model reproduces the observations well both in shape and amplitude.

Fofana and Beroual [1997] presents the same model as their 1996b paper with several key additions, including: (1) The value of resistance per unit length is made time varying by making the leader cross sectional area vary in time and by making the leader conductivity dependent upon current. (2) The direction of the leader propagation is random. (3) The corona streamers at the leader tip are taken into account. The electric field at the cathode, the front of corona streamers, and the front of leader tips is estimated using a hyperboloidal approximation (an inverse logarithmic relationship of electrode radius and gap length) [*Hutzler and Hutzler*, 1982]. Corona inception from the cathode is determined by Peek's formula, which is a function of pressure, temperature, and the electrode radius of curvature. The electric field in the corona region is considered to be constant [*e.g., Gallimberti*, 1979; *Goelian et al.*, 1997]. The length of the first corona is determined by the intersection of the voltage profiles before and after the

corona development. The first corona is then allowed to grow until the hyperboloidal field falls below the critical field for propagation.

A leader will grow in length, either from the cathode, the cathode leader (the primary leader connected to the cathode) or the space leader tips, if the field at the leader's tip is greater than the critical field. The field at the leader tip (hyperboloidal) is adjusted for the presence of corona streamers, and the leader radius is calculated using an empirical relationship proposed by *Hutzler and Hutzler* [1982]. The growth of leaders is governed by leader propagation velocity which is determined by the air density and the power injected to the leader head by the streamers, where the power is derived from the voltage and current determined by the RLC circuit. The propagation velocities of the positive and negative ends of the space leaders are different (positive is faster).

The following list is a summary of how the per unit length values of RLC for each process are determined.

- Streamer resistance: assumed to be the ratio of the electric field to the current flowing through all of the streamers. The value of the streamer electric field is assumed to be 1.5 MV/m.
- Leader resistance: non-LTE, controlled by ohmic heating and gas dynamic expansion, time-varying. Leader is cyclindrical with conductivity related to current and cross section.
- The leader resistance during final jump: drops sharply, described by a relation given by *Gallimberti* [1979] which depends on the channel resistance prior to the attachment.
- Channel resistance during 'return stroke': channel radius is kept constant by a balance of magnetic and kinetic forces, conductivity proportional to $T^{1.5}$.

- Inductances: end effects are ignored. The per unit length is approximated by familiar logarithmic equations which include external and internal inductance. Same calculation is used for all processes.
- Capacitance: calculated from a spherical approximation that depends on the voltage and distance to the ground plane.

3.4 Aleksandrov and Bazelyan [1996]

Aleksandrov and Bazelyan [1996] model the propagation of long positive streamers in air. Their model is based on the Poisson equation and continuity equations for charged particles (electrons, positive and negative ions) and neutral active particles (excited neutrals). Interactions accounted for by the model include: electron impact ionization, dissociative and three-body attachment of electrons to molecules, electron detachment from negative ions impacting other particles, excitation and quenching of electronically excited molecules, electron-ion and ion-ion recombinations, and photo-ionization. A total of 20 species were included, with 120 collisional processes that are important on short time intervals (about 10^{-6} s). Modeling is done for the case that the streamer radius is fixed, and for the case when the streamer radius is allowed to expand (due to increasing ionization radius and radial (transverse) component electric field.

3.5 Aleksandrov et al. [1997]

Aleksandrov et al. [1997] develop a kinetic model for the ionization processes in high-temperature air in a strong electric field. The model was used to study numerically the problem of the relaxation of the plasma properties in atmospheric-pressure air to a new steady state following an instantaneous change in the gas temperature between 300 and 1600 K. The main purpose of the paper was to estimate the response time for the leader plasma to clarify the dominant mechanisms of electron generation and loss in the leader channel, thereby allowing the

electric field in the leader to be related to the gas temperature. Modeling indicates that the reduced electric field decreases with increasing leader temperature.

3.6 Aleksandrov and Bazelyan [2000]

Aleksandrov and Bazelyan [2000] investigate step propagation in positive streamers in electronegative gases using a 1.5-D numerical model. The model was previously used in *Aleksandrov et al.* [1995], and *Aleksandrov and Bazelyan* [1996]. In the model, the streamer radius is constant and given a priori. The plasma parameters are averaged over the streamer cross section, and radial processes, such as diffusion, are neglected. The model is based on the Poisson equation and continuity equations for charged particles (electrons, positive and negative ions) and neutral active particles (excited neutrals). For air, over 200 ion-molecular processes are taken into account (different chemical reactions for different air molecules). The model is solved numerically using finite differences with an adaptive grid.

3.7 Alexandrov et al. [2001]

Alexandrov et al. [2001] examine the time evolution of the plasma parameters in a cross-section of plasma parameters of long leaders in air, such as the channel temperature, electric field, reaction rates, electron densities, and channel radius. They perform time-dependent modeling with allowance for the time-varying energy deposition in the leader channel, the channel expansion, and the non-equilibrium ionization kinetics in the plasma. In order to simplify the modeling, the evolution of the leader is modeled in two different phases: the initial phase and the main phase. The initial phase is the initial heating of the leader within about 10 cm of the leader head, which lasts for about 10 μs, and is governed primarily by processes occurring on times scales on the order of 10^{-7} s. The main phase beings about 30 cm from the leader head, where the channel reaches a temperature around 6000 K. The main phase describes

the channel evolution from about 30 μs after inception to 10 ms, and is governed by slower processes, such as the radial cooling of the channel through molecular heat conduction.

3.8 Gallimberti et al. [2002]

Gallimberti et al. [2002] summarizes many of the fundamental physical processes involved in the long air gap discharge, including the first ionization process, the first corona streamer inception, the formation of a stem, and the subsequent space leader. Many physical equations are given with which the processes can be discretised for modeling purposes. Much of the material focuses on positive discharges and is adapted from *Gallimberti* [1979], a paper that reviews nearly every aspect of the positive-polarity discharge and spark. In later sections of *Gallimberti et al.* [2002] (Section 3.6), the processes specific to the negative discharge are discussed, and much of this discussion appears to come from *Bacchiega et al.* [1994]. The following is a summary of the key physics identified in *Gallimberti et al.* [2002].

When the electric field exceeds a critical value in the active region (the region in which the electric field is at or above the critical value), electron avalanche breakdown will occur following the appearance of seed electrons. The seed electrons can be produced by many processes, such as photoionization, radioactive decay, or cosmic rays. The inception of corona requires that the number of ions produced by electron avalanche breakdown exceed a minimum value, N_{crit}. The number of ions is governed by the ionization and attachment coefficients, which themselves depend on the electric field. The minimum electric field, E_i, required to bring the ion number above N_{crit} can be determined using Peek's equation [*Peek*, 1929] given by:

$$E_i = E_0 \delta M \left(1 + \frac{K}{\sqrt{\delta R_{eq}}} \right) \qquad 2\text{-}1$$

where E_0 is the breakdown field (typically 3 MV m^{-1}), δ is the relative air density, R_{eq} is the equivalent radius of curvature of the electrode, and K and M are empirical constants (different forms of Peek's equation are used in different reports). Equation 2-1 is apparently valid for both positive and negative breakdown. Note that the value of E_0 can decrease for longer air gaps (greater than a few mm), where there is more distance for the electrons to gain energy.

A corona streamer consists of two regions: the streamer head, and the streamer channel. The streamer head, also called the active region, is where the electric field is greatest. Most of the ionization processes and luminous emissions occur in the streamer head. The streamer head has the following characteristics:

- it contains a net electrical charge
- its molecules have a rotational temperature not exceeding 330 K, and a vibrational temperature of 1000 K (vibrational temperature has a longer relaxation time)
- its electron energies are in the range of 5 to 15 eV
- it has an average electric field strength of 10 to 15 MV m^{-1}
- it has a head radius ranging from 10 to 30 μm, and an electron density on the order of 10^{21} m^{-3}

The streamer channel is where a conduction current exists that carries free electrons towards (for positive polarity) or away from (for negative polarity) the electrode. The streamer channel has the following characteristics:

- a radius on the order of 10 to 30 μm and an electron density (in short gaps) between 10^{19} and 10^{21} m^{-3}. The electron density can be much lower in long gaps where electron-electronegative attachment processes can play a more significant role.
- an electronic conduction current flowing in a resistive regime, $I = \pi a^2 \sigma E$.

The photons emitted by electron transitions (decays) in excited molecules produces, by photo-ionization, secondary electrons around the streamer head which lead to new avalanches if the electric field is suitable.

Equations are given in *Gallimberti et al*. [2002] to determine the number of ions in the streamer head as a function of voltage, position (in one dimension), streamer head radius, and energy loss and gain coefficients. Equations are given to determine the stability field in corona streamers, which is constant. The resulting potential profile (linear) can be compared to the pre-corona potential profile to determine the streamer extent, which is from the high-voltage electrode to the point where the two profiles intersect. The area between the two potential profiles is proportional to the streamer charge.

The next process of the discharge is the development of a pilot. The pilot forms at the root of the corona discharges and leads to the space stem. For the negative discharge, in which electrons move towards the cathode (away from the leader tip), the corona root is located ahead of (and separately from) the leader tip. The opposite is true for the positive discharge; the electrons flow away from the anode (away from the leader tip), and the root is essentially co-located with the anode or leader tip.

Gallimberti et al. [2002] refer to the model given by *Bacchiega et al.* [1994] as a possible qualitative description of the space stem development. The first corona streamers are a plasma channel of low conductivity ($\sim 10^{-4}$ S m^{-1}). Following the extinction of the current flow, the streamer plasma undergoes a classical relaxation process that tends to increase the local potential to that of the high-voltage electrode in order to reduce to zero the plasma electric field. The time during which the relaxation process takes place depends on the corona geometry and charge distribution. The potential at the old corona streamer front may increases sufficiently to create

the electric field necessary to launch negative corona (towards anode) and backwards positive corona (towards cathode). Figure 2 illustrates this view of the time evolution of the corona potential profile during the evolution of a space stem, with curves a through d showing:

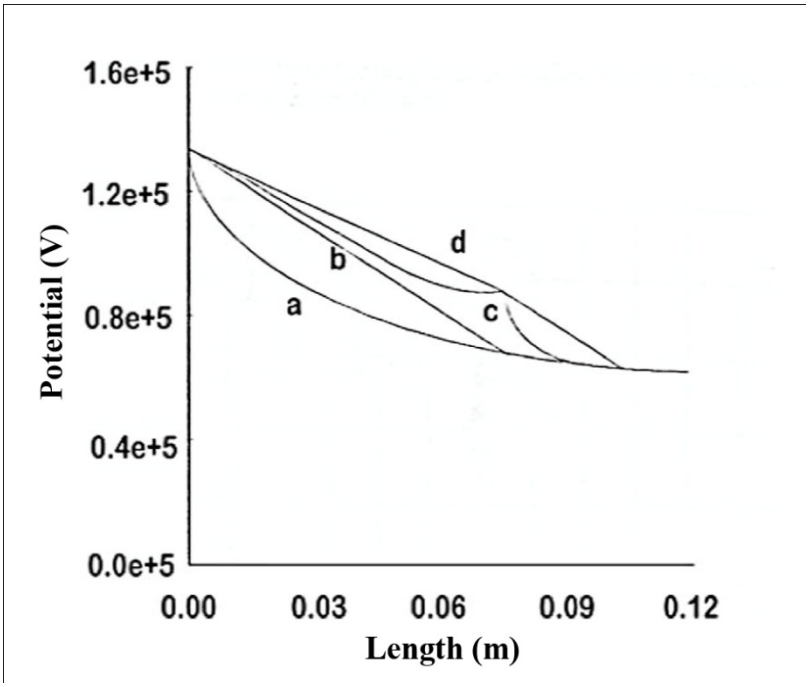

Figure 2. The evolution of the potential profile before (a) and after (b) negative corona development, during the relaxation process (c) and after the pilot formation (d). Taken from *Gallimberti et al.* [2002].

a) The initial distribution of the geometric potential (the potential between the hyperboloidal cathode and planar anode).

b) The linear potential distribution after corona streamers have formed (the electric field is assumed to be constant in the corona streamers). The length of the corona streamers extends from the cathode to the intersection of curves a and b.

c) The potential distribution during the relaxation process, where the front of the corona streamers has increased in potential relative to the surrounding plasma and gas.

d) The potential distribution after space stem formation at the intersection of c and d. Here the electric field increases sufficiently to form two corona streamers of opposite polarities. The electric field in these corona streamers is assumed to be constant, which results in the linear potential profile.

This process is modeled using a distributed RLC circuit with varying resistance determined by the ionic densities. It should be noted that in the model formulation of *Bacchiega et al.* [1994], the positive and negative streamers in the pilot begin simultaneously, which contradicts the observations of *Reess et al*. [1995], which show that the positive streamers supply the space stem with the negative charge needed to launch new negative corona streamers.

The corona streamer currents converge on the stem region and increase the local thermal energy, producing significant effects, including:

- a temperature increase of the gas and plasma by Joule heating from about 300 K to 1000 K.
- a hydrodynamic expansion and reduction in gas density
- an increase in the electron detachment of the negative ions due to the increase in temperature and reduced electric field
- a sharp increase the conductivity of the stem
- an increase in the electric field at the stem tips

These effects make possible the start of a second corona to drive the leader advancement. Typically the stem will move away from the cathode, and subsequent pilots will form downstream or in parallel (two or more pilots exist simultaneously). When the temperature in the stem reaches a critical temperature of 1500 K, negative ions abruptly release their captured

electrons. This causes a large and abrupt increase in the plasma conductivity, and the formation of a space leader.

The space leader appears as a thin luminous channel connecting corona regions to the high-voltage electrode. The leader cross-sectional area increases in time, and the longitudinal current is confined to a diameter between 0.5 mm and a 2-4 mm. Leader diameters are larger in longer gaps since there is more time for hydrodynamic expansion. The average electric field along the leader channel has been estimated to be on the order of 10^5 V m^{-1}, and it decreases with leader length. The ratio of light to current is essentially constant for all wavelengths. *Gallimberti et al.* [2002] then notes that mathematical models of the leader channel are very complex since they must incorporate thermodynamic and hydrodynamic process along with electrical processes. They point to a model developed by *Braginskii* [1958] in which the leader channel is represented by a thin core with constant thermodynamic properties, and a dense thin shell with varying properties.

The leader evolution is modeled assuming that the stem consists of three types of particles: electrons, ions, and neutral particles. Conservation of mass, momentum, and energy are invoked to describe the evolution of each species (specific ion, molecule, etc) along with the field and current density equations. The generalized systems are given for each conserved quantity. The temperature evolution of the stem is computed by solving two balance equations for thermal enthalpy and one for vibrational energy of gas molecules.

The extension speed of the leader is the ratio of the current to the per-unit-length charge needed for leader advancement, the latter of which is measured to range from 30 to 50 μC m^{-1}.

A system of energy conservation equations are used to derive expressions for the leader velocity and leader charge, and the Schokley-Ramo theorem is used to determine the leader current.

3.9 Morrow and Blackburn [2002]

Marrow and Blackburn [2002] calculate the details of streamer propagation over a 50 cm point to plane gap. The model they used was previously described in *Marrow and Lowke* [1979]. The modeling is based on continuity equations for electrons, positive ions and negative ions, coupled with Poisson's equation. The continuity equations account for impact-ionization, attachment, recombination, diffusion, and photoionization. Their modeling indicates that streamers will only extend to a length that is equivalent to the applied voltage divided by the critical electric field, which they assume is 3 MV m^{-1}.

3.10 Rakotonandrasan et al. [2008]

Rakotonandrasana et al. [2008] model the long negative discharge using a RLC equivalent electrical network that predicts the spatial and temporal evolution of spark current, power, energy, and velocity. The model is based on a similar RLC model for long positive discharges [*Fofana and Beroual*, 1996]. The *Rakotonandrasana et al.* model describes the different processes of propagation, such as the first corona, the pilot (the space stem and its cathode-directed positive leaders and anode-directed negative leaders), the space leader, and the junction of the space leader to the primary leader, and the final jump. At any given time step in the model, each process of the discharge is represented by RLC equivalent circuit with appropriate parameters (e.g., the resistance per unit length of a streamer is different than that of a leader). The impulse voltage applied is described by a bi-exponential equation with adjustable rise time,

fall time, and amplitude factor. The model inputs are the applied voltage waveform, the geometry of the electrodes, and the ambient air pressure and temperature.

The spatial location of the space stem, and thus the origin of the space leader is governed by the power injected at the head of the corona streamers, and the power is computed from the voltage and current determined by the RLC circuit. The direction of propagation is determined by a probabilistic law determined by *Hutzler and Hutzler* [1982] which assumes that the leader path should become more random (less axial) in a lower electric field. This aspect of the model is not well described.

Once the space leader attaches to and extends the cathode leader, corona streamers develop from the newly formed leader tip. The length of the streamers is determined by the same method as the first corona; graphical intersection of the potential before and after the leader forms. The transition from the free development phase to the final jump phase (attachment) occurs with the overall leader height is below the height to which an upward positive leader should form, the later being determined by an empirical relationship.

The model is tested for two experimentally observed cases, a 7-m discharge from *Les Renardieres Group* [1981], and a 16.7-m discharge from *Ortega et al.* [1994]. The model reasonably reproduces the overall features of the breakdown, such as the number of space leaders, and the overall gap traversal time. The model under-predicts the amount of current and apparent charge, especially for the 16.7-m discharge. The model shows promise, although it could probably use some refinement, and a more detailed description. More comparisons should be made to other observed discharges.

References

Aleksandrov, N. L., and E. M. Bazelyan (1996), Simulation of long-streamer propagation in air at atmospheric pressure, *J. Phys. D: Appl. Phys.*, *29*, 740-53.

Aleksandrov, N. L., and E. M. Bazelyan (1999), Ionization processes in spark discharge plasmas, *Plasma Sources Sci. Technol.*, *8*, 285-94.

Alecksandrov, N. L. and E. M. Bazelyan (2000), Step propagation of a streamer in an electronegative gas, *J. Exp. Theor. Phys.*, *91*, *4*, 724-35.

Aleksandrov, N. L., E. M. Bazelyan, I. V. Kochetov, and N. A. Dyatko (1997), The ionization kinetics and electric field in the leader channel in long air gaps, *J. Phys. D: APpl. Phys.*, *30*, 1616-24.

Aleksandrov, N. L., E. M. Bazelyan, A. M. Konchakov (2001), Plasma parameters in the channel of a long leader in air, *Plasm. Phys. Rep.*, *27*, *10*, 878-85.

Bacchiega, G., A. Gazzani, M. Bernardi, I. Gallimberti, and A. Bondiou-Clergerie (1994), Theoretical modeling of the laboratory negative stepped-leader, *Int. Conf. on. Lightning and Static Elec.*, Mannheim, Germany.

Bazelyan, E. M., and Y. P. Raizer (1998), *Spark Discharge*, CRC Press, Boca Raton, Fla.

Bazelyan, E. M, E. N. Brago, and I. S. Stekol'nikov (1961), The large reduction in mean breakdown gradients in long discharge gaps with an oblique-sloping voltage wave, *Sov. Phys.*, *5*.

Braginskii, S. I. (1958), Theory of the development of the spark channel, *Sov. Phys. JETP*, 34, 1068-74.

Carrara, G., and L. Thione (1976), Switching Surge Strength of Large Air Gaps: A Physical Approach, *IEEE Trans.*, Vol. PAS-95, *2*, pp. 512-524.

Domens, P. (1987), Contribution l'etude des descharges electriques dans les grands intervalles d'air, These de Doctorat d'Etat es sciences, University of Pau (France).

Domens, P., A. Gilbert, J. Dupuy, and B. Hutzler (1991), Propagation of the positive streamer-leader system in a 16.7 m rod-plane gap, *J. Phys. D Appl. Phys.*, *24*, 1748-57.

Dwyer, J. R., H. K. Rassoul, Z. Saleh, M. A. Uman, J. Jerauld, and J. A. Plumer (2005a), X-ray bursts produced by laboratory sparks in air, *Geophys. Res. Lett.*, *32*, L20809, doi:10.1029/2005GL024027.

Fofana, I., and A. Beroual (1995), Modeling of the leader current with an equivalent electrical network, *J. Phys. D: Appl. Phys.*, *28*(2), pp. 303-313.

Fofana, I., and A. Beroual (1996a), A new proposal for calculation of the leader velocity based on energy considerations, *J. Phys. D: Appl. Phys.*, *29*, pp. 691-96.

Fofana, I., and A. Beroual (1996b), A model for long air gap discharge using an equivalent electrical network, *IEEE Trans. Dielec. Elect. Ins.*, *3*(2), doi:10.1109/94.486779.

Fofana, I., and A. Beroual (1997), A predictive model of the positive discharge in long air gaps under pure oscillating impulse shapes, *J. Phys. D: Appl. Phys.*, 30, pp. 1653-67.

Gallimberti, I. (1979), The mechanism of long spark formation, *Journal de Physique C7, 40*, pp. 193-205,1979.

Gallimberti, I., G. Bacchiega, A. Bondiou-Clergerie, and P. Lalande (2002), Fundamental processes in long air gap discharges, *C. R. Physique, 3*, doi:10.1016/S1631-0705(02)01414-7.

Goelian, N., P. Lalande, A. Bondiou-Clergerie, G. L. Bacchiega, A. Gazzani, and I. Gallimberti (1997), A simplified model for the simulation of positive-spark development in long air gaps, *J. Phys. D: Appl. Phys*, *30*, 2441-52.

Gorin, B. N., V. I. Levitov, and A. V. Shkilev (1976), Some principles of leader discharge of air gaps with a strong non-uniform field, *IEE Conf. Publ.*, *143*, 274–278.

Hutzler, B. and D. Hutzler (1982), A model of the breakdown in large air gaps, EdF Bull. Etudes et Recherches, Sgrie B, No. 4, 1982, pp. 11-39.

Les Renardieres Group (1972), Research on long air gap discharges at Les Renardieres, *Electra*, *23*, 53-157.

Les Renardisres Group (1974), Research on long air gap at Les Renardieres - 1973 Results, *Electra*, *35*, July 1974, pp. 49-156.

Les Renardieres Group (1977), Positives discharges in long air gaps at Les Renardieres, *Electra*, *53*, pp. 31-153.

Les Renardieres Group (1981), Negative discharges in long air gaps at Les Renardieres, *Electra*, *74*, 67–216.

Loeb, L., and J. M. Meek (1941), The mechanism of the electric spark, Stanford University Press, Stanford, CA, 1941.

Morrow, R., and J. J. Lowke (1997), Streamer propagation in air, *J. Phys. D: Appl. Phys*, *30*, 614-27.

Morrow, R. and T. R. Blackburn (2002), The stepped nature of lightning, and the upward connecting streamer, *J. Phys. D: Appl. Phys.*, *35*, L69-L73.

Nguyen, C. V., A. P. J. van Deursen, E. J. M. van Heesch, G. J. J. Winands, and A. J. M. Pemen (2010), X-ray emission in streamer-corona plasma, *J. Phys. D: Appl. Phys.*, *43*, doi:10.1088/0022-3727/43/2/025202.

Nudnova, M. M, and A. Yu. Starikovskii (2008), Streamer head structure: role of ionization and photoionization, *J. Phys. D: Appl. Phys.*, *41*, doi:10.1088/0022-3727/41/23/234003.

Ortega, P. (1992), Comportement dielectrique des grands intervalles d'air soumis a des ondes de tension de polarite positives et negatives, These de Doctorat, University de Pau, Paris, France.

Ortega, P., et a1. (1991), Long air gap discharges under non standard positive impulse voltages, *Proc. 7th ISH*, Dresden pp 105-8.

Ortega, P., P. Domens, A. Gibert, B. Hutzler, and G. Riquel (1994), Performance of a 16.7 m air rod-plane gap under a negative switching impulse, *J. Phys. D Appl. Phys.*, *27*, doi:10.1088/0022-3727/27/11/019.

Ortega, P., F. Heilbronner, F. Ruhling, R. Diaz, and M. Rodiere (2005), Charge-voltage relationship of the first impulse corona, *J. Phys. D: Appl. Phys.*, 38, doi:10.1088/0022-3727/38/13/021.

Peek, F. W. (1929), Dielectric phenomena in high voltage engineering, New York, NY, USA, McGraw-Hill, pp. 52-80.

Pigini, A., G. Rizzi, R. Brambtlla, and E. Garbagnati (1979), Switching Impulse Strength of Very Large Air Gaps, ISH, Milan, paper No. 52.15.

Raether, H (1964), Electron avalanches and breakdown in gases, London, UK, Butterworths.

Rakotonandrasana, J. H., A. Beroual, and I. Fofana (2008), Modelling of the negative discharge in long air gaps under impulse voltages, *J. Phys. D: Appl. Phys.*, *41*, doi:10.1088/0022-3727/41/10/105210.

Reess, T., P. Ortega, A. Gibert, P. Domens, and P. Pignolet (1995), An experimental study of negative discharge in a 1.3 m point-plane air gap: The function of the space stem in the propagation mechanisms, *J. Phys. D Appl. Phys.*, *28*, doi:10.1088/00223727/28/11/011.

Rizk, A. M. F. (1989), A model for switching impulse leader inception and breakdown of long air-gaps, IEEE Trans. on Pow. Del, 4(1).

Thione, L. (1979), The Electric Strength of Air Gap Insulation, in *Surges in High Voltage Networks*, Edited by K. Ragaller, pp. 165-205.

Trichel, G. W. (1938), The mechanism of the negative point to plane corona near onset, *Phys. Rev.*, 54.

Wang, M. C., and E. E. Kunhardt (1990), Streamer dynamics, *Phys. Rev. A.*, *42*(4), 42-50.

Winands, G. J. J., Z. Liu, A. J. M. Pemen, E. J. M. van Heesch, and K. Yan (2008), Analysis of streamer properties in air as function of pulse and reactor parameters by ICCD photography, *J. Phys. D: Appl. Phys.*, *41*, doi:10.1088/0022-3727/41/23/234001.